BESSM, 2023, Vol 7, No 1, 44-51
https://doi.org/10.54987/bessm.v7i1.902

HIBISCUS PUBLISHER

BULLETIN OF ENVIRONMENTAL SCIENCE & SUSTAINABLE MANAGEMENT

Website: http://journal.hibiscuspublisher.com/index.php/BESSM/index

BESSM VOL 7 NO 1 2023 Azokeratin

# Substrate Inhibition Kinetics Models for Fitting the Growth Rate of Phenol by an Acclimatized Mixed Bacterial Consortia from an Anaerobic Batch Reactor

Ibrahim A. Allamin[1], Murtala Ya'u[2], Umar Abubakar Muhammad[3], Aisami Abubakar[4]*

[1]Department of Microbiology, Faculty of Science, University of Maiduguri P.M.B 1069 Maiduguri, Nigeria.
[2]Department of Biochemistry, Faculty of Basic Medical Sciences, College of Health Sciences, Bayero University Kano, PMB 3011 Gwarzo Road Kano, Nigeria.
[3]Department of Biological Sciences, Faculty of Science, Gombe State University, P.M.B 127, Tudun Wada, Gombe, Gombe State, Nigeria.
[4]Department of Biochemistry, Faculty of Science, Gombe State University, P.M.B 127, Tudun Wada, Gombe, Gombe State, Nigeria.

*Corresponding author:
Dr. Aisami Abubakar,
Department of Biochemistry,
Faculty of Science,
Gombe State University,
P.M.B 127, Tudun Wada,
Gombe,
Gombe State,
Nigeria.
Email: aaisami@gsu.edu.ng

**HISTORY**

Received: 1st May 2023
Received in revised form: 23rd June 2023
Accepted: 30th July 2023

**KEYWORDS**

Substrate Inhibition Kinetics
Phenol
Mixed Bacterial Consortia
Anaerobic Batch Reactor
Teissier

**ABSTRACT**

Particularly hazardous among the numerous synthetic chemicals made by mankind is phenol. A considerable number of the over 80,000 chemicals manufactured in the United States for industrial purposes are phenol and phenolic compounds, which enter the environment without undergoing sufficient safety evaluation. The potential utilization of phenol as a carbon source by several species of bacteria renders bioremediation of this hazardous substance an auspicious prospect. Our research revealed that the growth rate of acclimatized mixed bacterial consortia from an anaerobic batch reactor was considerably inhibited when exposed to extremely high quantities of phenol. The growth parameter-specific growth rate was determined by employing the modified Gompertz primary growth model. In the present investigation, we extend our previous work by employing multiple substrate inhibition kinetic models—including Monod, Teissier, Haldane, Yano and Koga, Aiba, Han and Levenspiel, Luong, Moser, Webb, and Hinshelwood—to further model the effect of substrate or phenol on the growth rate of the bacterium. All cases exhibit significant fits, with the exception of the Luong and Hinshelwood models. The Haldane model exhibited a higher degree of correspondence with the growth rate data obtained at various concentrations of phenol, as determined by the statistical tests. The designated values of the Haldane constants were maximal reduction rate, half saturation constant for maximal reduction and half inhibition constant which are symbolized by $\mu_{max}$, $K_s$ and $K_i$ were 0.157 $hr^{-1}$ (95% confidence interval 0.072 to 0.231), 32.042 mg/L (95% C.I. 14.603 to 49.480) and 234.095 mg/L (95% C.I. 181.83 to 286.17), respectively. The output of curve fitting interpolation should not be considered the true value, and the user should be duly informed of this as the true $\mu_{max}$ should be the point at which the slope's gradient becomes zero; in this instance, the value was 0.095 $h^{-1}$ at 50.1 mg/L phenol.

## INTRODUCTION

Synthetic chemicals created by humans, in particular, pose significant dangers to human health. Well over 80,000 chemicals were produced in the United States for use in industry, and many more compounds than that were discharged into the atmosphere without first undergoing enough testing to ensure their safety. Although it is correct that the toxicity of natural compounds and created chemicals cannot be compared, it is noteworthy to note that the five substances that are considered to be the most hazardous on Earth are all naturally occurring [1]. The phenol industrial pollutant is one of the most prevalent potentially

harmful compounds that are a direct result of the process of industrialization [2]. Phenol pollution of soils and water bodies has increased throughout the years, leading in worry for its removal from the environment.[3].

The acute symptoms of phenol poisoning can be caused by inhaling phenol or coming into direct contact with it through the skin. Phenol is known to be particularly irritating to the eyes, skin, and mucous membranes. A fast heartbeat, difficulty breathing, loss of coordination and tremor, fainting, and coma are some of the indications of intoxications in humans. Acute poisoning in humans can manifest itself in a variety of ways, including abnormal breathing patterns, trembling and weakening of the muscles, loss of balance, seizures, coma, and respiratory arrest. It has been observed that rodents, such as rats, mice, and rabbits, suffer from high levels of acute toxicity as a result of oral exposure to phenol [4–7].

A lack of energy, progressive weight loss, nausea, vertigo, excessive salivation, and a dark urine coloration are some of the chronic effects of phenol exposure in humans. In addition, impacts on the blood and liver, and also problems in the digestive system, have been observed. According to the findings of one research, after a subject was exposed to phenol by inhalation and skin contact, the subject experienced muscle pain and weakness, along with an enlarged liver and increased levels of liver enzymes. The use of phenol topically results in irritation and necrosis of the dermis. Arrhythmias in the heart have been observed in humans who were subjected to extraordinarily high amounts of phenol. When animals inhale phenol for extended periods of time, it has a toxic effect on their kidneys, central nervous system (CNS), liver, and lungs, and it can even affect their hearts.

The Reference Dose for phenol was determined to be 0.6 mg/kg/day after research on rats showed that fetal body weights were reduced. The reference dose is an oral exposure assessment for the public at large (as well as sensitive subgroups) which is anticipated to present no significant risk of adverse noncancerous outcomes over the course of a lifetime. This is the case because the reference dose is below the level at which cancer can develop. It is not an accurate measurement of risk; rather, it is a standard by which to judge the results. When exposures are higher than the reference dosage, there is a greater possibility that negative health outcomes will develop. A lifetime of contact in excess of the reference dosage does not necessarily result in the absence of detrimental effects on one's health in all cases. The EPA has low confidence in the study that was used to derive the reference dose because the dose was given via gavage in that study. But nevertheless, the data includes several supplementary studies (chronic, subchronic and reproductive/developmental), so the EPA has medium confidence in the reference dose overall [4,8–12].

Workers who were exposed to phenol reported slight increases in the likelihood of acquiring certain cancers; nevertheless, a connection between their phenol exposure and their higher cancer risk could not be established. However, dermal treatment of phenol may increase tumor growth and/or be a mild skin carcinogen in mice. Oral dosing of phenol did not cause malignancies in animals; however, dermal application of phenol did. In spite of this, the Environmental Protection Agency has classified phenol as "not classifiable as to human carcinogenicity" in Group D due to the paucity of knowledge regarding its carcinogenic effects in both humans and animals [13].

The biological method is the most popular treatment technology for phenol-containing wastewater around the world at the moment, and it has garnered a lot of attention as a result. In comparison to the physicochemical methods, the biological method has several advantages, including a straightforward pre-treatment process, a low initial investment in equipment, a high treatment capacity, the ability to be sustainable, and the absence of secondary pollution. Therefore, it is essential for the long-term growth of the environmental protection sector to conduct research on the methods of bioremediation for phenolic wastewater by microorganisms. To this day, a great number of bacteria capable of digesting phenol have been found [14–21].

Without accessibility to quantitative experimental data, it is not possible to build biological transformation processes and then optimize those processes. Several various mathematical models have been proposed in order to explain the metabolic characteristics of compounds when those chemicals are exposed to either pure cultures of microorganisms or wild populations of microorganisms. The relationship between the substrate concentration (S) and the specific growth rate ($\mu_{max}$) of a microbial colony is an important tool in biotechnology. The Monod equation is a typical tool that is used to characterize the relationship between growth and the rate of substrate consumption [22,23]. When a substrate, on the other hand, acts as an inhibitor of its own biodegradation, the original Monod model is rendered completely useless. In its place, the development of novel constant-carrying derivatives has taken place in order to facilitate substrate-related changes. The Haldane model is one that is used to represent substrate inhibition of growth or degradation rate, and it may be found in a wide variety of published works. Even though it has been demonstrated that alternative models are more accurate when taking into account a large number of substrate-inhibiting compounds all at once, such as phenol, this model is still widely employed. To illustrate this point, the Haldane model is not the only one currently available [24], In addition to the model, there have been numerous models that have been shown to be superior such as Luong [25,26] and Edward [27]. As a result of this, the Haldane may be rendered obsolete in some circumstances as a result of the utilization of the more extensive models that are currently available. It is not recommended to make haphazard use of the Haldane model without first doing exhaustive statistical analysis and attempting to fit other models to previously collected data on rate of growth or degradation. In this study, we continue the work by further modeling the influence of substrate or phenol on the growth rate of the bacterium by using different substrate inhibition kinetic models.

## MATERIALS AND METHODS

Data from Fig 1. from the growth of an acclimatized mixed bacterial consortia from an anaerobic batch reactor on phenol [28] was processed using the software Webplotdigitizer 2.5 [29]. It converts the scanned image into digital form and is used by a great number of scholars and is recognized for the accuracy it provides [30,31]. The specific maximum growth rate on phenol at various concentrations of phenol was obtained using a no lag modified logistics model as other primary growth models such as no lag modified Gompertz model failed to fit the growth data (published elsewhere). The ten models of inhibition kinetics are shown in **Table 1**.

**Table 1**. Various mathematical models developed for degradation kinetics involving substrate inhibition of phenol on an acclimatized mixed bacterial consortium from an anaerobic batch reactor.

| Author | Degradation Rate | Author |
|---|---|---|
| Monod | $\frac{\mu_{max}S}{S+K_s}$ | [32] |
| Haldane | $\frac{\mu_{max}S}{S+K_s+\left(\frac{S^2}{K_i}\right)}$ | [33] |
| Teissier | $\mu_{max}\left(1-exp\left(-\frac{S}{K_i}\right)-exp\left(\frac{S}{K_s}\right)\right)$ | [34] |
| Aiba | $\mu_{max}\frac{S}{K_s+S}exp\left(-\frac{S}{K_i}\right)$ | [35] |
| Yano and Koga | $\frac{\mu_{max}S}{S+K_s+\left(\frac{S^2}{K_i}\right)\left(1+\frac{S}{K}\right)}$ | [36] |
| Han and Levenspiel | $\mu_{max}\left(1-\left(\frac{S}{S_m}\right)\right)^n\left(\frac{S}{S+K_s\left(1-\left(\frac{S}{S_m}\right)\right)^m}\right)$ | [37] |
| Luong | $\mu_{max}\frac{S}{S+K_s}\left(1-\left(\frac{S}{S_m}\right)\right)^n$ | [38] |
| Moser | $\frac{\mu_{max}s^n}{K_s+s^n}$ | [39] |
| Webb | $\frac{\mu_{max}S\left(1+\frac{S}{K}\right)}{S+K_s+\frac{S^2}{K_i}}$ | [40] |
| Hinshelwood | $\mu_{max}\frac{S}{K_s+S}(1-K_pP)$ | [41] |

Note:
$\mu_{max}$ maximal specific growth rate
$K_s$ half saturation constant
$K_i$ inhibition constant
$S_m$ maximal concentration of substrate tolerated
$K_p$ product inhibition constant
m, n, K curve parameters
$S$ substrate concentration
$p$ product concentration

**Fitting of the data**

Fitting of the inhibition curves using various growth models was carried out using the CurveExpert Professional software (Version 1.6) by nonlinear regression utilizing the Marquardt algorithm.

**Statistical analysis**

The following statistical functions were utilized to determine the best models;

The RMSE allows number of parameters' penalty and was calculated using Equation 1, where $n$ illustrates the number of experimental data, where else $p$ is the number of parameters calculated by the model and experimental data and values predicted by the model are $Ob_i$ and $Pd_i$, respectively [42]. With the regression line approaching the data points, the root mean square error (RMSE) reduces due to the reduced error in the model. More accurate predictions are generated by a model that has a lower error rate. Comparable in magnitude to the dependent (outcome) variable, the RMSE values span an infinite number of positive infinities. The root mean square error (RMSE) can be employed to assess the extent of imprecision in a statistical model, including regression models. If a value is zero, it signifies that the predicted and actual values are an exact match. The model exhibits superior data fit and generates more precise predictions, as indicated by low RMSE values. In contrast, increased levels indicate a greater magnitude of errors and a reduced number of precise predictions.

$$RMSE = \sqrt{\frac{\sum_{i=1}^{n}(Pd_i - Ob_i)^2}{n-p}} \quad \text{(Eqn. 1)}$$

The $R^2$ value, also known as the coefficient of determination, was used in linear regression to select the model that provided the best fit. On the other hand, in the case of nonlinear regression, the $R^2$ does not provide a comparative analysis in situations in which the number of parameters in the various models varies. In order to get around this obstacle, the quality of the nonlinear models was determined by adjusting the $R^2$ value. $S_y^2$ is the total variance of the y-variable, while RMS stands for residual mean square. These two terms are used in the adjusted $R^2$ formula (Equations 2 and 3).

$$Adjusted\ (R^2) = 1 - \frac{RMS}{S_Y^2} \quad \text{(Eqn. 2)}$$

$$Adjusted\ (R^2) = 1 - \frac{(1-R^2)(n-1)}{(n-p-1)} \quad \text{(Eqn. 3)}$$

One can measure the relative quality of various statistical models for a given set of experimental data by using the Akaike Information Criterion (AIC). This criterion was developed by Akaike. Instead, data sets that have a large number of parameters or few values should utilize the AIC that has been corrected, which is denoted by the letter AICc [43]. The AICc was determined using the equation that is presented below (Equation 4).

$$AICc = 2p + n1n\left(\frac{RSS}{n}\right) + 2(p+1) + \frac{2(p+1)(p+2)}{n-p-2}$$
(Eqn. 4)

Another statistical measure that is founded on information theory is known as the Bayesian Information Criterion (BIC) (Equation 5), which can be compared to the AICc. Models with the lowest Bayesian information criterion (BIC) are typically preferred over those with higher BICs when choosing from a finite number of models. It has close ties to the Akaike information criteria and is partially based on the likelihood function (AIC). This error function imposes a harsher penalty on the number of parameters than the AIC does [44].

$$BIC = n.\ln\frac{RSS}{n} + p.\ln(n) \quad \text{(Eqn. 5)}$$

The Hannan–Quinn information criterion, often known as the HQC, is an additional error function approach that is based on the information theory (Equation 7). To evaluate how well a statistical model fits data, experts use the Hannan-Quinn information criterion (HQC). It is a common metric to employ when choosing one model over another. In contrast to the LLF, it is connected to Akaike's information criterion. The HQC, like the AIC, includes a penalty function for the total number of model parameters, however it is significantly bigger than the value assigned by the AIC because the equation contains the *ln ln n* term [45];

$$HQC = n \times ln\frac{RSS}{n} + 2 \times p \times ln(\ln n) \quad \text{(Eqn. 7)}$$

Both BF and AF were utilized in an effort to evaluate the appropriateness of the models. In order to get a correlation of 1 between the anticipated value and the observed value, the Bias Factor needs to be equal to 1. The Bias Factor and Accuracy Factor originates from predictive microbiology under the food microbiology field and have found applications in modelling

microbial growth that leads to food spoilage [46–53]. A fail-safe model is indicated when the value of the Bias Factor (Equation 8) is greater than 1, and a fail-negative model is indicated when the value of the Bias Factor is less than 1. When compared to 1, a value of Accuracy that is less than 1 indicates a less accurate prediction (Equation 9).

$$Bias\ factor = 10\left(\sum_{i=1}^{n} log\frac{(Pd_i/Ob_i)}{n}\right) \quad \text{(Eqn. 8)}$$

$$Accuracy\ factor = 10\left(\sum_{i=1}^{n} log\frac{|(Pd_i/Ob_i)|}{n}\right) \quad \text{(Eqn. 9)}$$

Another parameter-penalized model is MPSD. The Marquardt's percent standard deviation (MPSD). This error function distribution follows the geometric mean error which allows for the penalty to the number of parameters of a model (Equation 10).

$$MPSD = 100\sqrt{\frac{1}{n-p}\sum_{i=1}^{n}\left(\frac{Ob_i - Pd_i}{Ob_i}\right)^2} \quad \text{(Eqn. 10)}$$

where $p$ is the number of parameters, $n$ is the number of experimental data, $Ob_i$ is the experimental data, and $Pd_i$ is the value predicted by the model.

## RESULTS AND DISCUSSION

In this study, the specific maximum growth rate on phenol ($\mu_m$) was first obtained using the no lag modified logistics model (**Fig. 1**). The results of the RMSE, AICc, adjusted$R^2$, F-test, and bias and accuracy factor comparisons demonstrate that the Haldane model is the most accurate and precise of the kinetic models considered (**Table 2**). The resultant fittings (**Figs 2** to **11**) demonstrate satisfactory fit except for the Monod and Moser models.

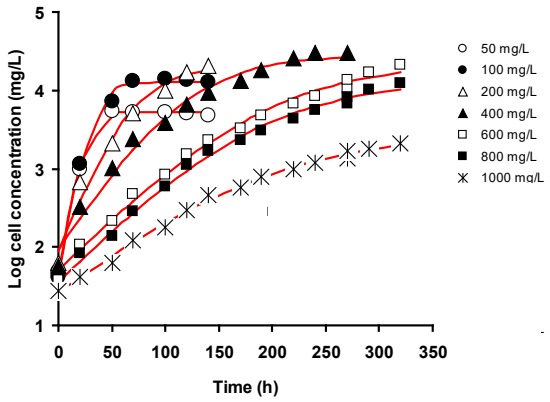


**Fig 1.** The growth curves of an acclimatized mixed bacterial consortia from an anaerobic batch reactor on various concentrations of phenol as modelled using the no lag modified Logistics model.

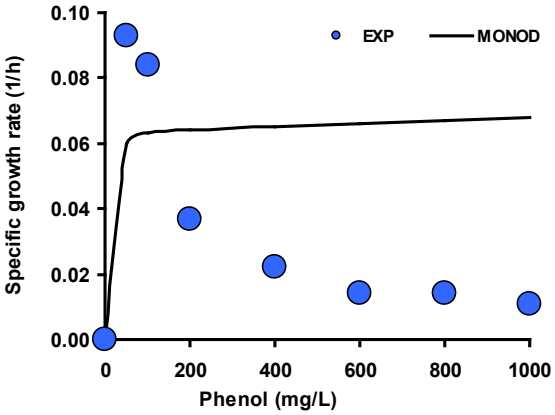


**Fig 2.**The particular growth data were fitted with respect to phenol concentration using the model of Monod.

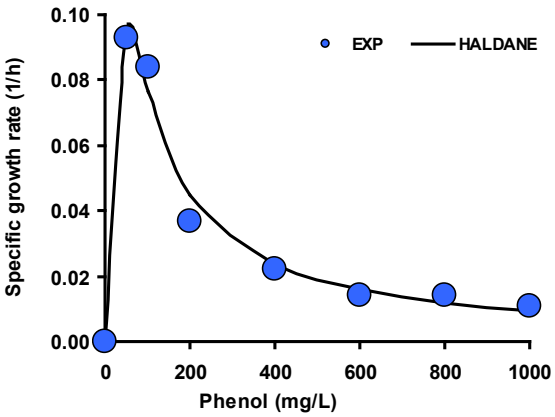


**Fig 3.** The particular growth data were fitted with respect to phenol concentration using the model of Haldane.

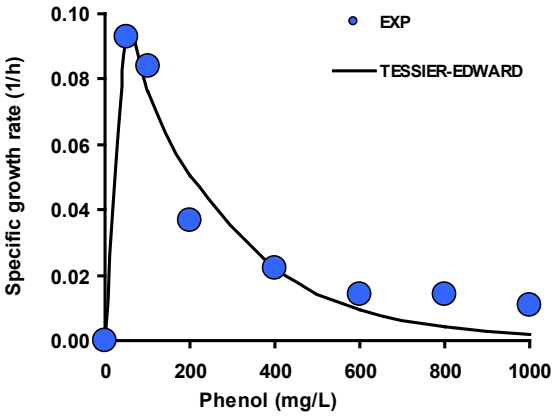


**Fig 4.** The particular growth data were fitted with respect to phenol concentration using the model of Teissier.

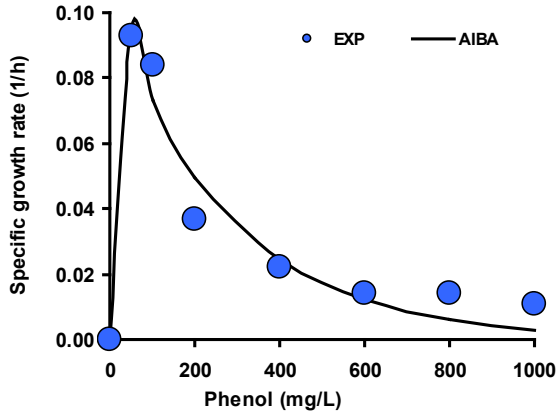


**Fig 5.** The particular growth data were fitted with respect to phenol concentration using the model of Aiba.

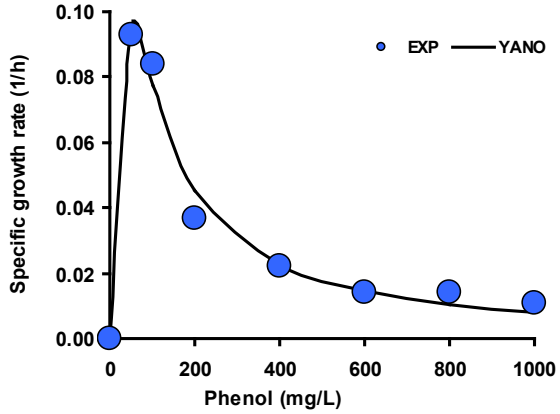


**Fig 6.** The particular growth data were fitted with respect to phenol concentration using the model of Yano and Koga.

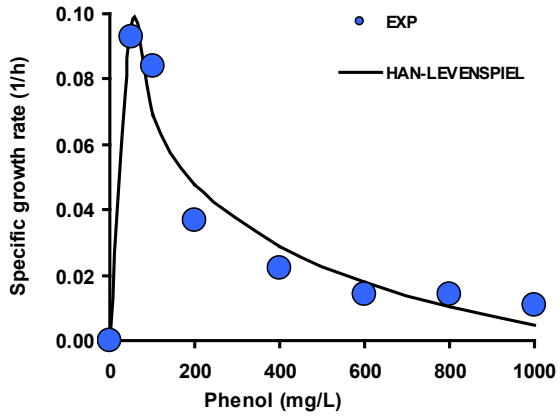


**Fig 7.** The particular growth data were fitted with respect to phenol concentration using the model of Han and Levenspiel.

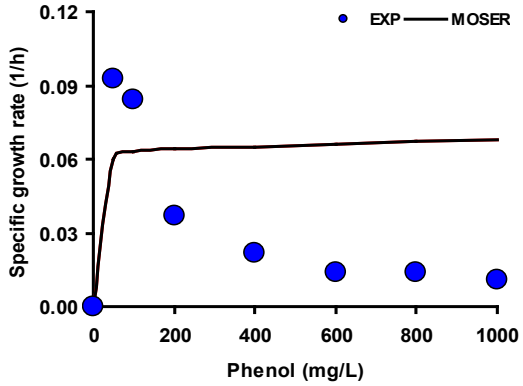


**Fig 8.** The particular growth data were fitted with respect to phenol concentration using the model of Moser.

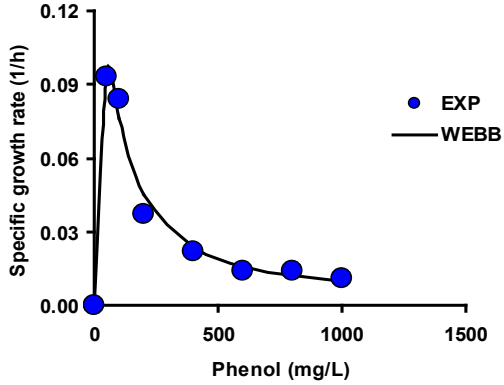


**Fig 9.** The particular growth data were fitted with respect to phenol concentration using the model of Webb.

**Table 1.** Statistical analysis of the various fitting models.

| Model | p | RMSE | adR2 | MPSD | AICc | BIC | HQC | BF | AF |
|---|---|---|---|---|---|---|---|---|---|
| Luong | 4 | n.a. | n.a. | n.a. | n.a. | n.a. | n.a. | n.a. | n.a. |
| Yano | 4 | 0.006 | 0.963 | 26.39 | -39.96 | -79.65 | -82.11 | 0.95 | 1.13 |
| Tessier-Edward | 3 | 0.009 | 0.918 | 245.12 | -51.15 | -72.24 | -74.09 | 0.68 | 1.60 |
| Aiba | 3 | 0.009 | 0.919 | 130.50 | -51.55 | -72.64 | -74.49 | 0.78 | 1.42 |
| Haldane | 3 | 0.005 | 0.971 | 15.04 | -60.31 | -81.41 | -83.25 | 1.00 | 1.11 |
| Monod | 2 | 0.046 | -3.859 | 70.46 | -35.46 | -47.30 | -48.53 | 2.08 | 2.49 |
| Han and Levenspiel | 5 | 0.012 | 0.800 | 79.74 | 27.98 | -67.62 | -70.70 | 0.94 | 1.30 |
| Moser | 3 | 0.077 | -5.696 | 77.18 | -17.53 | -38.62 | -40.47 | 2.08 | 2.49 |
| Hinshlewood | 4 | n.a. | n.a. | n.a. | n.a. | n.a. | n.a. | n.a. | n.a. |
| Webb | 4 | 0.007 | 0.946 | 16.68 | -37.12 | -76.80 | -79.26 | 1.00 | 1.11 |

Note:
*p* no of parameters
RMSE Root Mean Square Error
AdjR$^2$ Adjusted Coefficient of determination
BF Bias factor
AF Accuracy factor
n.a. not available

The designated values of the Haldane constants were maximal reduction rate, half saturation constant for maximal reduction and half inhibition constant which are symbolized by $\mu_{max}$, $K_s$ and $K_i$ were 0.157 hr$^{-1}$ (95% confidence interval 0.072 to 0.231), 32.042 mg/L (95% C.I. 14.603 to 49.480) and 234.095 mg/L (95% C.I. 181.83 to 286.17), respectively. The output of curve fitting interpolation should not be considered the true value, and the user should be duly informed of this as the true $\mu_{max}$ should be the point at which the slope's gradient becomes zero; in this instance, the value was 0.095 h$^{-1}$ at 50.1 mg/L phenol. The equation for the

Haldane model using the values obtained from the fitting is as follows;

$$\frac{0.157S}{S + 32.042 + \left(\frac{S^2}{234.095}\right)}$$

Models like Luong's, Teissier's, and Hans Levenspiel's have been developed to account for the occurrences in which the growth rate approaches zero at very high substrate concentrations where the earlier Monod model could not be used [54]. Overly high concentrations of substrates can have toxic and repressive effects on microbes, stunting their growth. Much of the current use of the Haldane model for modelling the effect of toxic xenobiotics to xenobiotic-degrading bacteria centres predominantly to phenol-degrading microorganisms [55–62]. This is followed by Teissier [63,64,64–66]. It appears that other models were found to be less reported and the reason for this is that in numerous cases only the Haldane model was utilized to model the effect of phenol on the growth or degradation rate of microorganisms on phenol.

In 1930, Haldane presented his model, now known as the Haldane model. The model is thought of as a development of the Monod model. The model includes a third constant, $K_i$, to account for substrate concentration-dependent inhibition of the specific growth rate. The substrate concentration at which the specific growth rate is half the maximum growth rate absent inhibition is equal to the inhibition constant or $K_s$. Hazardous substrate may slow an organism's specific growth rate at high substrate concentrations. The model can deal with both hazardous and non-hazardous substrates. The Haldane model's strength lies in its ability to characterize all stages of the kinetics of growth rate. The Haldane model was widely utilized because it well described growth rate at both low and high substrate concentration. Before the Haldane model becomes in popular use, the classical Monod model is the most often utilized model.

Jacques Monod first proposed the Monod model in 1942 [67] to explain the correlation between specific growth rate and substrate consumption rate in a bioreactor. Although they are quite similar in appearance, the Michaelis-Menten equation and the Monod equation are based on theory rather than observation. Similar to the Michaelis-Menten expression for enzyme kinetics, the Monod equation for the specific growth rate can be expressed in terms of constants. Methods given for calculating $v_{max}$ and $K_m$ for an enzyme reaction can, in theory, also be used to calculate $\mu_{max}$ and $K_S$. Substrate concentration alone or together with biomass concentration can be used to define the model in its various versions. Specifically, $X$ is biomass concentration, $K_s$ half saturation constant, specific bacterial growth rate, and $\mu_{max}$ is the maximum bacterial growth rate. There is no change in either the maximum growth rate or the half saturation constant of bacteria. In the bioreactor, the Monod model presumes that there is only a single substrate restricting growth (Monod, 1942). Kong lists several restrictions [68] on the usefulness of the Monod model [69]. At high substrate concentrations, the first restriction becomes apparent. Maximum specific growth rate is not affected by substrate concentration at high concentration. The second restriction appears when the concentration of the substrate is low. Growth at low substrate concentrations is substrate dependent. Third, the Monod model is inapplicable when the substrate is inhibited [70–72]. Similar to the Michaelis-Menten kinetics model, at low substrate concentrations, the growth rate approaches a first-order with respect to substrate concentrations whilst at elevated substrate concentrations, the growth rate approaches a zero-order with respect to substrate concentrations. For the Haldane and many substrates inhibition at high concentrations of substrate, the downward slope of the growth rate indicates a negative order of reaction. In many xenobiotics or hazardous compounds bioremediation works, toxic substrates that inhibit bacterial growth and consumption of substrates means that the Monod models will not be useful and the other substrate inhibition models are needed [73–77].

## CONCLUSION

In this work, we found that an acclimatized mixed bacterial consortium from an anaerobic batch reactor 's growth rate was significantly impeded at exceedingly high concentrations of phenol, and the majority of discriminatory statistical findings acquired indicated that the Haldane model more accurately represented the growth rate data at various concentrations of phenol. This study demonstrated that the popular Haldane model is often used due to its ability to model inhibitory effects of toxicant, especially phenol to the growth rate of microorganisms.

## REFERENCE

1. Özkara A, Akyil D, Konuk M. Pesticides, Environmental Pollution, and Health. In: Larramendy M, Soloneski S, editors. Environmental Health Risk - Hazardous Factors to Living Species [Internet]. InTech; 2016 [cited 2020 Jul 17]. Available from: http://www.intechopen.com/books/environmental-health-risk-hazardous-factors-to-living-species/pesticides-environmental-pollution-and-health
2. VanDoren PM. The Effects of Exposure to “Synthetic” Chemicals on Human Health: A Review. Risk Anal [Internet]. 1996 Jun [cited 2020 Jul 17];16(3):367–76. Available from: http://doi.wiley.com/10.1111/j.1539-6924.1996.tb01471.x
3. Ayeni O. A preliminary assessment of phenol contamination of Isebo River in south-western Nigeria. Greener J Phys Sci. 2014;4(2):30–7.
4. Bruce RM, Santodonato J, Neal MW. Summary Review of the Health Effects Associated With Phenol. Toxicol Ind Health. 1987 Oct 1;3(4):535–68.
5. Strikwold M, Spenkelink B, Woutersen RA, Rietjens IMCM, Punt A. Combining in vitro embryotoxicity data with physiologically based kinetic (PBK) modelling to define in vivo dose–response curves for developmental toxicity of phenol in rat and human. Arch Toxicol. 2013 Sep 1;87(9):1709–23.
6. Kottuparambil S, Kim YJ, Choi H, Kim MS, Park A, Park J, et al. A rapid phenol toxicity test based on photosynthesis and movement of the freshwater flagellate, Euglena agilis Carter. Aquat Toxicol. 2014 Oct 1;155:9–14.
7. Mohanta VL, Mishra BK. Occurrence and fate of phenolic compounds in groundwater and their associated risks. In: Legacy, Pathogenic and Emerging Contaminants in the Environment. CRC Press; 2021.
8. Kim JS, Chin P. Acute and chronic toxicity of phenol to mysid, Archaeomysis kokuboi. Korean J Fish Aquat Sci. 1995;28(1):87–97.
9. Abd Gami A, Shukor A, Yunus M, Abdul Khalil K, Dahalan FA, Khalid A, et al. Phenol and phenolic compounds toxicity. J Environ Microbiol Toxicol. 2014;2(1):11–23.
10. Gami AA, Shukor MY, Khalil KA, Dahalan FA, Khalid A, Ahmad SA. Phenol and its toxicity. J Environ Microbiol Toxicol. 2014;2(1):11–23.
11. Dhatwalia VK, Nanda M. Biodegradation of phenol: Mechanisms and applications. Toxicity and Waste Management Using Bioremediation. 2015. 198–214 p.
12. Duan W, Meng F, Cui H, Lin Y, Wang G, Wu J. Ecotoxicity of phenol and cresols to aquatic organisms: A review. Ecotoxicol Environ Saf. 2018;157:441–56.
13. US EPA R 05. Human Health Noncarcinogen Fact Sheet for Phenol: (Human Health Noncarcinogen - fish ingestion only), Wisconsin Department of Natural Resources [Internet]. 2015 [cited

2023 Jan 30]. Available from: https://www.epa.gov/gliclearinghouse/human-health-noncarcinogen-fact-sheet-phenol-human-health-noncarcinogen-fish-0
14. Kujur RRA, Das SK. Pseudomonas phenolilytica sp. nov., a novel phenol-degrading bacterium. Arch Microbiol. 2022 May 14;204(6):320.
15. Rusnam, Gusmanizar N, Rahman MF, Yasid NA. Characterization of a Molybdenum-reducing and Phenol-degrading Pseudomonas sp. strain Neni-4 from soils in West Sumatera, Indonesia. Bull Environ Sci Sustain Manag E-ISSN 2716-5353. 2022 Jul 31;6(1):1–8.
16. Hanafee N, Salleh NAM, Ahmad SA, Saada WZ, Yusof MT. Characterization of phenol-degrading fungi isolated from industrial waste water in Malaysia. Asia-Pac J Mol Biol Biotechnol. 2019;27(2):35–43.
17. Aisami A, Yasid NA, Johari WLW, Shukor MY. Estimation of the Q10 value; the temperature coefficient for the growth of *Pseudomonas* sp. aq5-04 on phenol. Bioremediation Sci Technol Res. 2017 Jul 31;5(1):24–6.
18. Szilveszter S, Fikó DR, Máthé I, Felföldi T, Ráduly B. Kinetic characterization of a new phenol degrading Acinetobacter towneri strain isolated from landfill leachate treating bioreactor. World J Microbiol Biotechnol. 2023 Jan 17;39(3):79.
19. Mousa A. Isolation and Characterization of Phenol degrading Bacteria from Wastewater. Int J Biol Phys Chem Stud. 2023 Sep 10;5:17–24.
20. Bandi SS, Mallisetty R, Veluru S, Hamzah HT, Poiba VR, Srikanth R. Isolation, identification and optimization of potential phenol degrading bacterial strain P7 using Gen III microlog. AIP Conf Proc. 2023 Sep 13;2764(1):020007.
21. Sandhyarani R, Mishra S. Isolation and characterization of phenol degrading organism, optimization using doehlert design. Desalination Water Treat. 2019;148:351–62.
22. Kiviharju K, Salonen K, Leisola M, Eerikäinen T. Modeling and simulation of Streptomyces peucetius var. caesius N47 cultivation and ε-rhodomycinone production with kinetic equations and neural networks. J Biotechnol. 2006;126(3):365–73.
23. Shokrollahzadeh S, Bonakdarpour B, Vahabzadeh F, Sanati M. Growth kinetics and Pho84 phosphate transporter activity of Saccharomyces cerevisiae under phosphate-limited conditions. J Ind Microbiol Biotechnol. 2007;34(1):17–25.
24. Arif NM, Ahmad SA, Syed MA, Shukor MY. Isolation and characterization of a phenol-degrading *Rhodococcus* sp. strain AQ5NOL 2 KCTC 11961BP. J Basic Microbiol. 2013;53(1):9–19.
25. Hamitouche AE, Bendjama Z, Amrane A, Kaouah F, Hamane D. Relevance of the Luong model to describe the biodegradation of phenol by mixed culture in a batch reactor. Ann Microbiol. 2012;62(2):581–6.
26. Nickzad A, Mogharei A, Monazzami A, Jamshidian H, Vahabzadeh F. Biodegradation of phenol by Ralstonia eutropha in a Kissiris-immobilized cell bioreactor. Water Environ Res. 2012;84(8):626–34.
27. Saravanan P, Pakshirajan K, Saha P. Batch growth kinetics of an indigenous mixed microbial culture utilizing m-cresol as the sole carbon source. J Hazard Mater. 2009;162(1):476–81.
28. Firozjaee T, Najafpour G, Asgari A, Bakhshi Z, Pishgar R, Mousavi N. Phenol Biodegradation Kinetics in an Anaerobic Batch Reactor. 2012.
29. Rohatgi A. WebPlotDigitizer. http://arohatgi.info/WebPlotDigitizer/app/ Accessed June 2 2014.; 2015.
30. Halmi MIE, Shukor MS, Johari WLW, Shukor MY. Modeling the growth curves of *Acinetobacter* sp. strain DRY12 grown on diesel. J Environ Bioremediation Toxicol. 2014;2(1):33–7.
31. Khare KS, Phelan Jr FR. Quantitative comparison of atomistic simulations with experiment for a cross-linked epoxy: A specific volume–cooling rate analysis. Macromolecules. 2018;51(2):564–75.
32. Monod J. The Growth of Bacterial Cultures. Annu Rev Microbiol. 1949;3(1):371–94.
33. Boon B, Laudelout H. Kinetics of nitrite oxidation by Nitrobacter winogradskyi. Biochem J. 1962;85:440–7.
34. Teissier G. Growth of bacterial populations and the available substrate concentration. Rev Sci Instrum. 1942;3208:209–14.
35. Aiba S, Shoda M, Nagatani M. Kinetics of product inhibition in alcohol fermentation. Biotechnol Bioeng. 1968 Nov 1;10(6):845–64.
36. Yano T, Koga S. Dynamic behavior of the chemostat subject to substrate inhibition. Biotechnol Bioeng. 1969 Mar 1;11(2):139–53.
37. Han K, Levenspiel O. Extended Monod kinetics for substrate, product, and cell inhibition. Biotechnol Bioeng. 1988;32(4):430–7.
38. Luong JHT. Generalization of monod kinetics for analysis of growth data with substrate inhibition. Biotechnol Bioeng. 1987;29(2):242–8.
39. Moser A. Kinetics of batch fermentations. In: Rehm HJ, Reed G, editors. Biotechnology. VCH Verlagsgesellschaft mbH, Weinheim; 1985. p. 243–83.
40. Webb JLeyden. Enzyme and metabolic inhibitors [Internet]. New York: Academic Press; 1963. 984 p. Available from: https://www.biodiversitylibrary.org/bibliography/7320
41. Hinshelwood CN. The chemical kinetics of the bacterial cell. Clarendon Press, Gloucestershire, UK; 1946.
42. Wayman M, Tseng MC. Inhibition-threshold substrate concentrations. Biotechnol Bioeng. 1976;18(3):383–7.
43. Akaike H. Making statistical thinking more productive. Ann Inst Stat Math. 2010;62(1):3–9.
44. Kass RE, Raftery AE. Bayes Factors. J Am Stat Assoc. 1995 Jun 1;90(430):773–95.
45. Burnham KP, Anderson DR. Model Selection and Multimodel Inference: A Practical Information-Theoretic Approach. Springer Science & Business Media; 2002. 528 p.
46. Ross T, McMeekin TA. Predictive microbiology. Int J Food Microbiol. 1994;23(3–4):241–64.
47. Zhou K, George SM, Métris A, Li PL, Baranyi J. Lag phase of Salmonella enterica under osmotic stress conditions. Appl Environ Microbiol. 2011;77(5):1758–62.
48. Zhao J, Gao J, Chen F, Ren F, Dai R, Liu Y, et al. Modeling and predicting the effect of temperature on the growth of *Proteus mirabilis* in chicken. J Microbiol Methods. 2014;99(1):38–43.
49. Velugoti PR, Bohra LK, Juneja VK, Huang L, Wesseling AL, Subbiah J, et al. Dynamic model for predicting growth of Salmonella spp. in ground sterile pork. Food Microbiol. 2011;28(4):796–803.
50. McElroy DM, Jaykus LA, Foegeding PM. Validation and analysis of modeled predictions of growth of Bacillus cereus spores in boiled rice. J Food Prot. 2000;63(2):268–72.
51. Kowalik J, Lobacz A, Tarczynska AS, Ziajka S. Graphie validation of growth models for Listeria monocytogenes in milk during storage. Milchwissenschaft. 2012;67(1):38–42.
52. Jung SH, Park SJ, Chun HH, Song KB. Effects of combined treatment of aqueous chlorine dioxide and fumaric acid on the microbial growth in fresh-cut paprika (capsicum annuum L.). J Appl Biol Chem. 2014;57(1):83–7.
53. Huang L, Hwang CA, Phillips J. Evaluating the Effect of Temperature on Microbial Growth Rate-The Ratkowsky and a Bělehrádek-Type Models. J Food Sci. 2011;76(8):M547–57.
54. Saravanan P, Pakshirajan K, Saha P. Growth kinetics of an indigenous mixed microbial consortium during phenol degradation in a batch reactor. Bioresour Technol. 2008;99(1):205–9.
55. Kotturi G, Robinson CW, Inniss WE. Phenol degradation by a psychrotrophic strain of *Pseudomonas putida*. Appl Microbiol Biotechnol. 1991;34(4):539–43.
56. Bai J, Wen JP, Li HM, Jiang Y. Kinetic modeling of growth and biodegradation of phenol and m-cresol using *Alcaligenes faecalis*. Process Biochem. 2007;42(4):510–7.
57. Agarry SE, Audu TOK, Solomon BO. Substrate inhibition kinetics of phenol degradation by *Pseudomonas fluorescence* from steady state and wash-out data. Int J Environ Sci Technol. 2009;6(3):443–50.
58. Long TR, Zhang Z, Zhuan RX. Biodegradation of phenol by a novel isolated bacterium *Pseudomonas* sp. CN-6. Tumu Jianzhu Yu Huanjing GongchengJournal Civ Archit Environ Eng. 2010;32(5):82–7.
59. Liu J, Wang Q, Yan J, Qin X, Li L, Xu W, et al. Isolation and characterization of a novel phenol degrading bacterial strain WUST-C1. Ind Eng Chem Res. 2013;52(1):258–65.
60. Basak SP, Sarkar P, Pal P. Isolation and characterization of phenol utilizing bacteria from industrial effluent-contaminated soil and kinetic evaluation of their biodegradation potential. J Environ Sci

Health - Part ToxicHazardous Subst Environ Eng. 2014;49(1):67–77.
61. Ding C, Wang Z, Cai W, Zhou Q, Zhou J. Biodegradation of phenol with *Candida tropicalis* isolated from aerobic granules. Fresenius Environ Bull. 2014;23(3 A):887–95.
62. Mohanty SS, Jena HM. Biodegradation of phenol by free and immobilized cells of a novel *Pseudomonas* sp. nbm11. Braz J Chem Eng. 2017 Mar;34:75–84.
63. Agarry SE, Solomon BO. Kinetics of batch microbial degradation of phenols by indigenous *Pseudomonas fluorescence*. Int J Environ Sci Technol. 2008;5(2):223–32.
64. Agarry SE, Solomon BO, Layokun SK. Substrate inhibition kinetics of phenol degradation by binary mixed culture of *Pseudomonas aeruginosa* and *Pseudomonas fluorescence* from steady state and wash- out data. Afr J Biotechnol. 2008;7(21):3927–33.
65. Begum SS, Radha KV. Investigating the performance of inverse fluidized bed biofilm reactor for phenol biodegradation using *Pseudomonas fluorescence*. In: Proceedings of the International Conference on Green Technology and Environmental Conservation, GTEC-2011. 2011. p. 130–6.
66. Halmi MIE, Shukor MS, Johari WLW, Shukor MY. Mathematical modelling of the degradation kinetics of *Bacillus cereus* grown on phenol. J Environ Bioremediation Toxicol. 2014;2(1):1–5.
67. Monod J. The Growth of Bacterial Cultures. Annu Rev Microbiol. 1949;3(1):371–94.
68. Muloiwa M, Nyende-Byakika S, Dinka M. Comparison of unstructured kinetic bacterial growth models. South Afr J Chem Eng. 2020 Jul 1;33:141–50.
69. Kong JD. Modeling Microbial Dynamics: Effects on Environmental and Human Health [Internet] [PhD Thesis]. [Canada]: University of Alberta; 2017 [cited 2023 Nov 11]. Available from: https://era.library.ualberta.ca/items/0191844e-958e-49fb-bc42-feec802a29ea/view/b06920dd-a80e-427e-b7b9-4aa9433c579e/Kong_Jude_D_201708_PhD.pdf
70. Mulchandani A, Luong JHT, Groom C. Substrate inhibition kinetics for microbial growth and synthesis of poly-β-hydroxybutyric acid by *Alcaligenes eutrophus* ATCC 17697. Appl Microbiol Biotechnol. 1989;30(1):11–7.
71. Teissier G. Growth of bacterial populations and the available substrate concentration. Rev Sci Instrum. 1942;3208:209–14.
72. Han K, Levenspiel O. Extended Monod kinetics for substrate, product, and cell inhibition. Biotechnol Bioeng. 1988;32(4):430–7.
73. Yakasai HM, Babandi A, Uba G. Inhibition Kinetics Study of Molybdenum Reduction by *Pantoea* sp. strain HMY-P4. J Environ Microbiol Toxicol. 2020 Dec 31;8(2):24–9.
74. Yakasai HM, Babandi A, Manogaran M. Modelling the Kinetics Molybdenum Reduction Rate by *Morganella* sp. J Environ Microbiol Toxicol. 2020 Dec 31;8(2):18–23.
75. Uba G, Abubakar A, Ibrahim S. Optimization of Process Conditions for Effective Degradation of Azo Blue Dye by Streptomyces sp. DJP15: A Secondary Modelling Approac. Bull Environ Sci Sustain Manag. 2021 Dec 31;5(2):28–32.
76. Othman AR, Rahim MBHA. Modelling the Growth Inhibition Kinetics of Rhodotorula sp. strain MBH23 (KCTC 11960BP) on Acrylamide. Bioremediation Sci Technol Res. 2019 Dec 28;7(2):20–5.
77. Habibi A, Vahabzadeh F. Degradation of formaldehyde at high concentrations by phenol-adapted *Ralstonia eutropha* closely related to pink-pigmented facultative methylotrophs. J Environ Sci Health - Part ToxicHazardous Subst Environ Eng. 2013;48(3):279–92.